Andreev Reflection in Graphene Nanoribbons

Diego Rainis[1], F. Taddei[1], F. Dolcini[1], M. Polini[1] and R. Fazio[1,2]

[1] *NEST-CNR-INFM and Scuola Normale Superiore, I-56126 Pisa, Italy*

[2] *International School for Advanced Studies (SISSA), Via Beirut 2-4, I-34014 Trieste, Italy*

Abstract

We study Andreev reflection in graphene nanoribbon/superconductor hybrid junctions. By using a tight-binding approach and the scattering formalism we show that finite-size effects lead to notable differences with respect to the bulk graphene case [1]. Conservation of pseudoparity, a quantum number characterizing the ribbon states, yields at subgap voltages either a suppression of Andreev reflection when the ribbon has an even number of sites in the transverse direction or perfect Andreev reflection when the ribbon has an odd number of sites [2]. In the former case the suppression of Andreev reflection induces an insulating behavior even when the junction is biased; electron conduction can however be restored by applying a gate voltage.

What is Andreev Reflection? 1

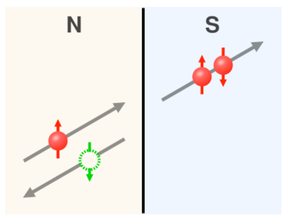

Fig.1 Schematic representation of Andreev (Retro-) Reflection at the interface between a Metal (left) and a Superconductor (right).

Andreev Reflection (AR) [3]: electron → hole conversion at the interface between a normal metal and a superconductor (electron 1 into hole 3 in Fig. 2). The missing charge of $2e$ enters the superconductor as a Cooper pair in the ground state (labeled 4 in Fig. 2).

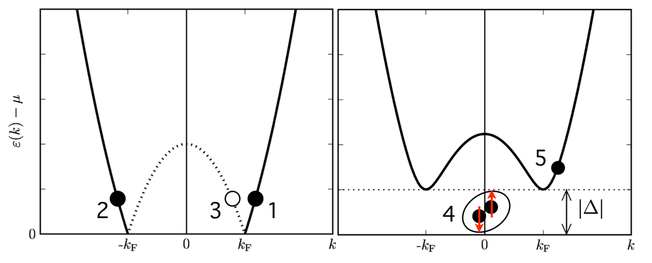

Fig.2 Left: dispersion relation of electron-like (solid line) and hole-like (dotted line) excitations in the metal region. Right: dispersion relation in the superconducting region; for energies lower than the gap $|\Delta|$ no excitations are available, and one can transfer charge only by injecting Cooper pairs.

- At energies below the superconducting gap, $E < |\Delta|$, Andreev reflection is the only process that contributes to the conductance G of the interface, since normal transmission of electrons is prohibited (no excitation states available in the superconductor side). For every Andreev process a charge of $2e$ is transmitted, thus we have $G \propto 2R_A$ (R_A is the Andreev reflection coefficient).
- At energies $E > |\Delta|$ normal transmission becomes possible (electron 5 in Fig. 2), so that the conductance has two contributions. Actually, normal transmission of electrons is favorite on Andreev reflection, and the Andreev reflection coefficient drops rapidly to zero with increasing energies.

What is Graphene? 2

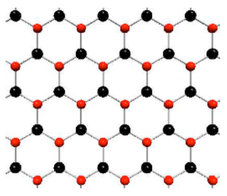

Graphene [4] is a flat monolayer of Carbon atoms arranged in a two-dimensional (2D) honeycomb lattice. Since the honeycomb lattice is a non-Bravais lattice, a sublattice degree-of-freedom has to be introduced: it is termed *pseudospin* and its two components refer to the A or B sublattices.

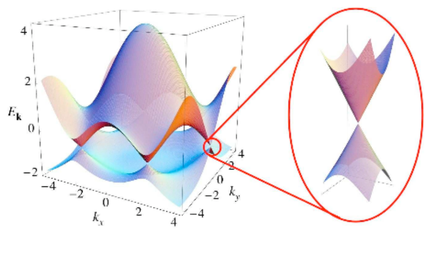

There are six points in k-space where valence and conduction bands touch each other, but because of symmetry considerations, it is sufficient to consider only two of these points, which are called *valleys*. At each valley, graphene's dispersion relation at low energies has a conical structure, that is, the energy-momentum relation is linear, and thus electronic excitations behave as massless (chiral) particles.

References

[1] C.W.J. Beenakker, Phys. Rev. Lett. **97**, 067007 (2006); C.W.J. Beenakker, arXiv:0710.3848v2.
[2] D. Rainis *et al.*, arXiv:0806.4475.
[3] A.F. Andreev, Sov. Phys. JETP **19**, 1228 (1964).
[4] A.K. Geim and K.S. Novoselov, Nature Mater. **6**, 183 (2007); A.K. Geim and A.H. MacDonald, Phys. Today **60**(8), 35 (2007); A.H. Castro Neto *et al.*, arXiv:0709.1163v2.
[5] K. Wakabayashi and T. Aoki, Int. J. Mod. Phys. B **16**, 4897 (2002); A.R. Akhmerov *et al.*, Phys. Rev. B **77**, 205416 (2008); A. Cresti *et al.*, Phys. Rev. B **77**, 233402 (2008); J. Nakabayashi, D. Yamamoto, and S. Kurihara, arXiv:0806.4978.

Andreev Reflection in Bulk Graphene 3

It has been shown [1] that the peculiar band structure of graphene gives rise to the appearance of *specular* Andreev reflection, a novel type of AR that is absent in ordinary metal/SC interfaces. By moving the Fermi level it is possible to choose the reflected hole to be in the valence band or in the conduction band, and to switch from the regime of ordinary AR to the one of specular AR.

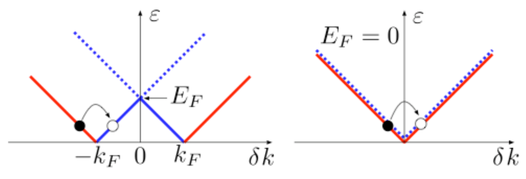

Fig.3 Specular Andreev reection (right panel) happens if an electron in the conduction band is converted into a hole in the valence band. In the usual case (left panel), instead, electron and hole both lie in the conduction band. The momentum k of the hole is fixed by conservation laws, but the velocity ($\propto \partial E/\partial k$) of the hole is opposite in the two cases. Figures taken from [1].

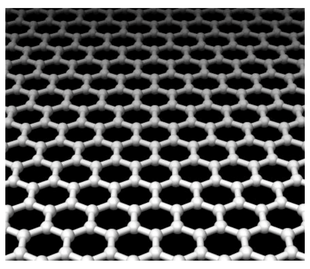

Most of the theoretical analysis carried out so far in literature describe the graphene sheet as an infinite (or semi-infinite) 2D plane, and identify two energy scales relevant for transport, namely the superconducting gap $\Delta_0 = |\Delta|$ and the displacement E_F of the Fermi level from the Dirac level (the energy at which valence and conduction bands touch each other).

In graphene nanoribbons (GNRs), however, the finite size W of the sample yields an additional energy scale $\delta \propto W^{-1}$, characterizing the mean energy spacing between the ribbon sub-bands. We have

$$W = 10 \text{ nm} \div 1\ \mu\text{m} \quad \Rightarrow \quad \delta = 3 \text{ meV} \div 300 \text{ meV}$$

and thus δ is larger than (or of the same order of) the typical superconducting gap $\Delta_0 \lesssim 1$ meV. As a consequence, δ is expected to play an important role in electron transport and AR in graphene.

Nanoribbon Eigenstates 4

We consider the case of a ribbon with zigzag edges, which has been shown to represent fairly well the behavior of an arbitrarily shaped edge. We model the GNR by means of the tight-binding Hamiltonian

$$\hat{\mathcal{H}} = -\gamma \sum_{\langle \boldsymbol{i},\boldsymbol{j} \rangle} \hat{c}^\dagger_{\boldsymbol{i}} \hat{c}_{\boldsymbol{j}} + U \sum_{\boldsymbol{i}} \hat{c}^\dagger_{\boldsymbol{i}} \hat{c}_{\boldsymbol{i}} \,, \qquad (1)$$

where $\gamma \simeq 2.8$ eV is the hopping energy between nearest-neighbor sites $\langle \boldsymbol{i},\boldsymbol{j} \rangle$ on the honeycomb lattice, and U accounts for a constant electrostatic energy, which can be controlled by a gate voltage.

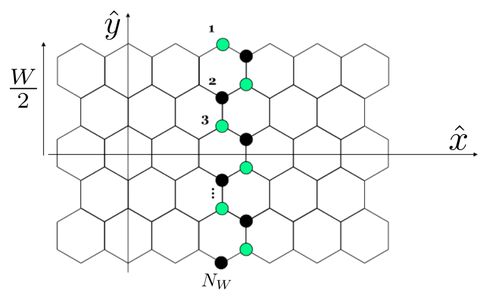

We find that the eigenfunctions of the Hamiltonian (1) which obey to the appropriate boundary conditions are of the form:

$$\Psi_{A(B)}(x,y) = e^{ik_x} x_{A(B)}(x) \cdot \begin{pmatrix} \sin[k_y(W/2+y)] \\ \eta \ \sin[k_y(W/2-y)] \end{pmatrix} , \qquad (2)$$

where $x_{A(B)}(x)$ is the coordinate of the $A(B)$ site of the unit cell located at (x,y) and W is the width of the ribbon. We see that Ψ is made up by:

- A plane-wave factor along the longitudinal direction $\hat{x}$, which comes from translational invariance and is labeled by the quantum number k_x ;
- A spinor $\begin{pmatrix} \Phi_A \\ \Phi_B \end{pmatrix}$ along the transverse direction $\hat{y}$, which turns out to be labeled by a quantum number $\eta = \pm 1$, termed *pseudoparity*, that tells us whether the transverse "average" wave function $(\Phi_A + \Phi_B)/2$ is even or odd with respect to the ribbon center $y = 0$. The quantum number k_y labeling the transverse modes is related to k_x through the tight-binding equations and the boundary conditions.

Thus, because of the boundary conditions, the eigenstates of finite-size nanoribbons are labeled by the pseudoparity rather than by the pseudospin .

Pseudoparity 5

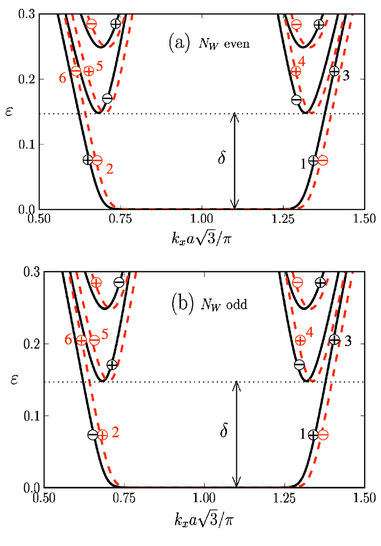

Fig.4 For the even N_W case we find that:

- Electron or hole states at fixed valley and sub-band have all the same pseudoparity;
- Electron states and hole states at the same energy and momentum have opposite pseudoparity;
- Pseudoparity values (± 1) alternate from one sub-band to the other;
- States at the same energy but from opposite valleys have the same pseudoparity.

Fig.5 For odd N_W we have instead that:

- States at the same energy but from opposite valleys have opposite pseudoparity.

This difference between even and odd N_W, together with a selection rule on pseudoparity quantum number, is responsible for different behaviors in the conductance for the two cases.

Calculation of the Conductance 6

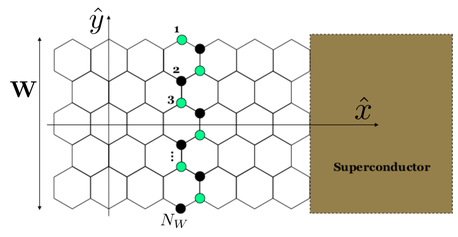

The coupling between electrons and holes in the superconductor is is accounted for by the Bogoliubov-de Gennes Hamiltonian, with pairing amplitude Δ:

$$\mathcal{H}_{\text{BdG}} = \begin{pmatrix} \mathcal{H} - E_F & \Delta \\ \Delta^* & E_F - \mathcal{H}^* \end{pmatrix} , \qquad (3)$$

where $\mathcal{H}$ is the particle Hamiltonian (1), and E_F gives the position of the Fermi level in the superconducting region.

We then obtain the Hamiltonian of the whole junction through the Dyson's equation, and by means of appropriate Green's functions we calculate the probability for all different processes that can take place in the junction (e.g. the reflection coefficient R and the Andreev reflection coefficient R_A).

Finally, the zero-temperature differential conductance is given by

$$G(V) = \frac{4e^2}{h} \left[N(V) - R(V) + R_A(V) \right] , \qquad (4)$$

where V is the bias voltage applied across the junction. The prefactor 4 is due to spin and valley degeneracies, whereas $N(V)$ is the number of transverse propagating modes ("open channels") available at energy eV measured from the Fermi level E_F.

Numerical Results 7

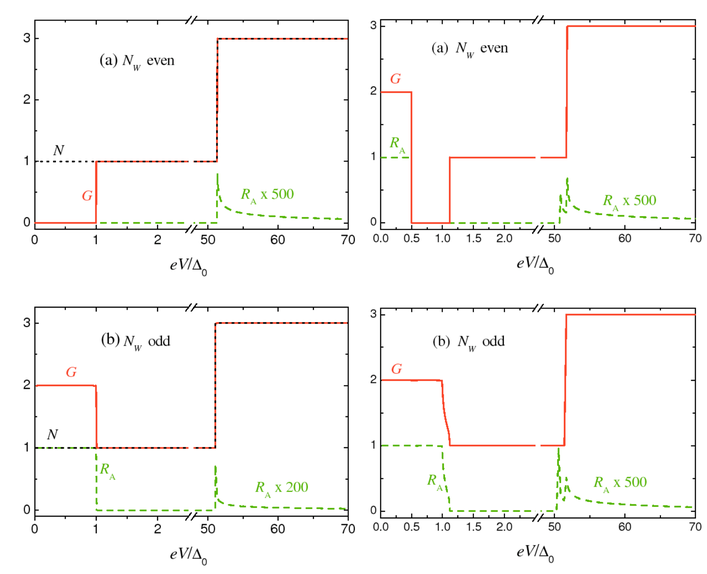

Fig.6 Conductance G (red) and Andreev Reflection coefficient R_A (green) for the GNR-SC junction as a function of the applied bias potential. We have considered here the realistic case $W \simeq 50$ nm, for which $\delta \simeq 52$ meV $\gg \Delta_0$. Left: for the undoped case ($E_F = 0$, Fermi level at the Dirac point) we observe opposite behaviors for the even N_W case (above) and the odd N_W case (below). In the former case, Andreev reflection and thus conductance at subgap voltages are suppressed to zero because of pseudospin conservation. R_A remains zero until $eV = \delta$, where new channels open up, while G becomes finite at $eV = \Delta_0$, when transmission becomes possible. In the odd case instead, Andreev reflection is allowed by pseudospin conservation and thus we get $R_A = 1$ and $G = 2$ (in units of $4e^2/h$) below the gap. Right: by applying a gate voltage U one can shift rigidly the electron and hole dispersion relations and restore a finite R_A for the even case in an energy window $[0 : U]$. In the odd case we don't obtain any substantial modification (below).

By looking at the pseudoparity configuration within the ribbon bands of Figg. 4 and 5, one can explain the observed behaviors of Fig. 6.

- Let's consider a right-propagating electron, indicated in Fig. 4 by label 1, incoming from the GNR region. It can be scattered into a left-propagating electron or into a left-propagating hole, labeled by 2. Since the pairing amplitude is constant along the transverse direction, it cannot couple states with different pseudoparity (*i.e.* the pseudoparity of an electron impinging onto the interface cannot be flipped). Thus, electron 1 can only be scattered into an outgoing left-propagating electron, that is, normal reflection takes place while Andreev reflection is forbidden. Instead, at energies larger than δ, for an incoming electron, say 3, there are also available hole states with the same pseudoparity (4 or 6): Andreev reflection is possible.
- In the odd N_W case (Fig. 5), thanks to the different pseudoparity configuration, the incoming electron 1 can only be scattered into the hole 2, that is, Andreev reflection process is allowed and takes place with probability 1. At higher energies the situation is similar, because for an electron of given pseudoparity there is always a counter-propagating hole with the same pseudoparity.

CONCLUSIONS

In summary, we have studied Andreev reflection in graphene nanoribbon/superconductor hybrid junctions. We have reported analytical expressions for the eigenfunctions of the tight-binding Hamiltonian describing the graphene ribbon, which are valid at arbitrary energy and carry explicitly a definite pseudoparity. The selection rule stemming from this quantum number has strong implications on transport through the junction.

For nanoribbons with an even number of sites in the transverse direction we have found a complete suppression of Andreev reflection in a wide range of energies when the Fermi energy lies at the Dirac level. This implies zero conductance at subgap voltages, but it can however be restored by applying a finite gate potential, opening up potential technological applications of these hybrid junctions as electron transistors as well as nanorefrigerators. In contrast, in the case of ribbons with an odd number of sites we have found perfect Andreev reflection at subgap voltages and an abrupt suppression of it above the gap.

The study of non-ideal edges, realistic interfaces, and bulk disorder is postponed to a future publication. The role of electron-electron interactions and/or next nearest-neighbor hopping, which also has not been addressed here, can be qualitatively understood as follows: these effects have been shown to lead to the opening of a gap Δ_g at the Dirac level, which is however typically much smaller than δ. Our conclusions thus remain valid for a large range of energies even when these effects are taken into account.